

QTL mapping for petiole shape in non-heading Chinese cabbage

Zhongwen Chen^{1#}, Aimei Bai^{1#}, Xinya Wang¹, Tianzi Zhao¹, Feixue Zhang², Yan Li¹, Tongkun Liu¹, Xilin Hou¹ and Ying Li^{1*}

¹ State Key Laboratory of Crop Genetics & Germplasm Enhancement and Utilization, Engineering Research Center of Germplasm Enhancement and Utilization of Horticulture Crops, Ministry of Education, College of Horticulture, Nanjing Agricultural University, Nanjing 210095, China

² Huzhou Academy of Agricultural Sciences, Institute of Horticulture, Huzhou 313000, China

Authors contributed equally: Zhongwen Chen, Aimei Bai

* Corresponding author, E-mail: yingli@njau.edu.cn

Abstract

Non-heading Chinese cabbage (NHCC) is an important leafy vegetable in China. Petiole shape is crucial for NHCC, and cultivating diverse and abundant petiole shapes is essential to meet consumer demand. Understanding the genetic mechanism for petiole shape is significant for variety innovation. Petiole length (PL), petiole width (PW), and petiole thickness (PT) emerge as cardinal phenotypic proxies for shape characterization. In this study, 127 RILs from Wutacai and Erqing were used for QTL mapping. Genetic analysis revealed that PL, PW, and PT are dominant traits controlled by multiple genes. To obtain comprehensive and accurate QTL, phenotypic data collected from three locations and BLUP values were used for QTL mapping. 19 stable QTLs were detected and distributed as four for PL, seven for PW, and eight for PT. The QTL on chromosomes A03 and A04 were detected in all three traits and shared similar physical positions. The QTL *qPL.A03.1*, *qPW.A03.1*, and *qPT.A03.1* showed negative additive effects, signifying the contributions for slender, wider, and thicker petiole from the Erqing allele. The QTL *qPL.A04.1* and *qPT.A04.1* exhibited positive additive effects, whereas *qPW.A04.1* showed negative additive effect, which suggested that the Wutacai allele contributed to slender and thicker petiole and contributions from Erqing allele led to wider petiole. Candidate genes analysis in parental lines revealed that *BcIAA31* and *BcBOP2* were the promise candidate genes in QTL on chromosomes A03 and A04. These findings advance mechanistic understanding of petiole morphogenesis and establish a molecular toolkit for marker-assisted pyramiding of optimal petiole traits in NHCC breeding programs.

Citation: Chen Z, Bai A, Wang X, Zhao T, Zhang F, et al. 2025. QTL mapping for petiole shape in non-heading Chinese cabbage. *Vegetable Research* 5: e020 <https://doi.org/10.48130/vegres-0025-0014>

Introduction

Non-heading Chinese cabbage (*Brassica rapa* ssp. *chinensis*; NHCC) is a popular leafy vegetable in China and widely cultivated in the middle and lower reaches of the Yangtze River. Leaves are the predominant edible organ of NHCC. NHCC has abundant germplasm resources and can be divided into six variants according to the genome, displaying various leaf morphologies^[1]. Leaves can be divided into two parts: the photosynthetic blade (lamina) and the structurally specialized petiole. Petioles can provide mechanical support and transfer water and nutrients from stem to leaves, processes critical for blade morphogenesis and photosynthetic efficiency^[2]. Blades have traditionally dominated varietal selection criteria in breeding programs. Conventional breeding strategies have primarily focused on reducing petiole specific gravity while expanding blade area, resulting in cultivars characterized by short, narrow, and thin petioles to maximize photosynthetic efficiency and foliar yield. Notably, petioles have emerged as versatile raw materials for value-added processing, including industrial-scale production of pickled foods, dehydrated products, and plant-based meat analogues, which result in breeding objectives toward developing longer, wider, and thicker petioles to meet processing industry requirements. Furthermore, petiole morphology constitutes a critical appearance quality trait for NHCC. Cultivar diversification through the development of shape-variable petioles (e.g., flattened, grooved, or cylindrical geometries) could cater to heterogeneous consumer aesthetics while optimizing processing adaptability.

Petiole shape is determined by petiole length (PL), petiole width (PW), and petiole thickness (PT), which is controlled by cell elongation and cell division^[3]. Previous studies reported that

genetics, light, and phytohormones played crucial roles in the development of petiole. Light contributes to petiole elongation, while phytochrome regulation performs core roles in regulating petiole elongation during a seeding stage in many species^[4]. The development of leaf petioles in *Arabidopsis* is regulated by a phytochrome-mediated mechanism. The *phy b* mutants in *Arabidopsis* show longer petiole^[5]. Low light intensity can induce plants to extend the petiole and shade avoidance for adoptive growth. Photoperiod also plays a role in regulating petiole elongation. Under the short day length (SD), the petiole exhibits shorter cell length and fewer cells^[6]. After the emergence of the petiole, the petiole cell elongation is affected by photoperiod, whereas the cell number in the petiole is independent^[6]. Moreover, light can also activate brassinosteroid (BR) biosynthesis to promote petiole development^[7]. Far-red light can induce auxin and gibberellin accumulation and function in petiole growth^[8]. However, only a limited genetic model and a few genes associated with PL, PW, and PT were revealed in previous studies.

In soybeans, short petiole length is controlled by single recessive genes^[9]. In *Arabidopsis*, the inheritance analysis revealed that *phyB*, *GAI*, *GA1*, and *ROT3* function in cell elongation and proliferation in petioles^[10–12]. In spinach, the BC₁ population is adapted to QTL mapping, and three QTLs controlling petiole length were obtained^[13]. In broccoli, a total of 23 QTL for PL is identified using a DH population. Five QTLs showed a positive additive effect and contributed to 3.93%–20.02% of the trait^[14]. The inheritance of petiole characteristics in *Brassica rapa* was revealed in 1986^[15]. The study illustrated that PL and PT were controlled by a small number of genes, and the dominant genes showed important effects^[15]. In

Brassica rapa, a total of four QTLs related to petiole are identified by a DH population^[13]. Li et al. revealed three QTLs related to PL on A01 and A03 chromosomes using an F₂ population^[16]. Our previous study also revealed PL, PW, and PT were controlled by multiple genes. A total of four QTLs for PL, two QTLs for PW, and three QTLs for petiole shape were explored using an RIL population, developed by Suzhouqing & Maertou^[17]. However, different populations developed from different parental lines may lead to different QTLs for the same phenotypes. Obtaining comprehensive QTL can contribute to identifying more key genes, clarifying the molecular regulatory network, and developing effective and widely applicable molecular markers for breeding.

In this study, Wutacai and Erqing, which showed significant differences in petiole shape, were adopted to identify the QTL for petiole. PL, PW, and PT were used to characterize petioles' shape. Phenotypic data was collected from three locations to perform genetic analysis and calculate broad sense heritability by constructing a mixed linear model. To obtain comprehensive and accurate QTL, BLUPs and all of the phenotypic data were utilized for QTL mapping using the MQM method. Co-localized QTL between PL, PW, and PT were annotated, and possible candidate genes were screened. The study provides a genetic basis to reveal the genetic mechanisms and develop valuable and effective molecular markers for petiole shape in NHCC.

Materials and methods

Plant material

Wutacai as the female parent and Erqing as the male parent were adopted to construct an F_{7:8} recombinant inbred lines (RIL) population comprising 127 lines. Wutacai produced slimmer, narrow, and thin petioles, and Erqing exhibited dumpy, wide, and thick petioles. Parental lines, F₁ hybrid, and RIL population were planted at the Baima Research Station (BRS, 31°35' N and 119°09' E) of Nanjing Agricultural University in Jiangsu Province, Jurong Experimental

Station (JES, 31°56' N and 119°16' E) of Nanjing Agricultural University in Jiangsu Province, and Huzhou Academy of Agricultural Sciences Experimental Station (HES, 30°90' N and 120°08' E) in Zhejiang Province. The RIL population was planted in three plot replications to reduce microenvironmental variation at HES. All plants were directly sowed in September 2021, and phenotypic data were evaluated at about 98 d after germination. The experiment was conducted using a randomized complete block design (RCBD).

Phenotypic data collection

The largest leaves were selected to measure the length, width, and thickness of the petiole (Fig. 1a). The petiole length (PL) was measured from the bottommost tip of the petiole to overlap between the petiole and lamina. The width of the bottommost tip in the petiole was considered the final petiole width (PW). The thickest region of the petiole was considered the final petiole thick (PT). Three plants for each line were studied as biological replications.

Statistical analysis of phenotypic data

The phenotypic data was collected from three locations. Genotypes, environments, and repeat-in environments were adopted to estimate the best mixed linear model of PL, PW, and PT using the *R/lme4* package. Analysis of variance (ANOVA) was utilized for PL, PW, and PT to estimate the variance of genotypes and environmental effects. Best linear unbiased predictors (BLUPs) were obtained from the mixed linear model with genotypes, environments, and repeats in environments as random factors, and they were further used for QTL mapping. The broad sense heritability (H^2) was estimated by the formula, $H^2 = \sigma_g^2 / (\sigma_g^2 + \sigma_{ge}^2/E + \sigma_e^2/E \times R)$.

QTL mapping

The genetic linkage map has been constructed in previous studies^[18]. QTL mapping was performed using *R/qtl* and *R/qtl2* packages^[19,20]. Simple marker analysis (SMA) was utilized for preliminary QTL mapping. Multiple-QTL mapping (MQM) method was also employed to improve the accuracy of the results of the QTL mapping. The LOD threshold was determined by 1,000

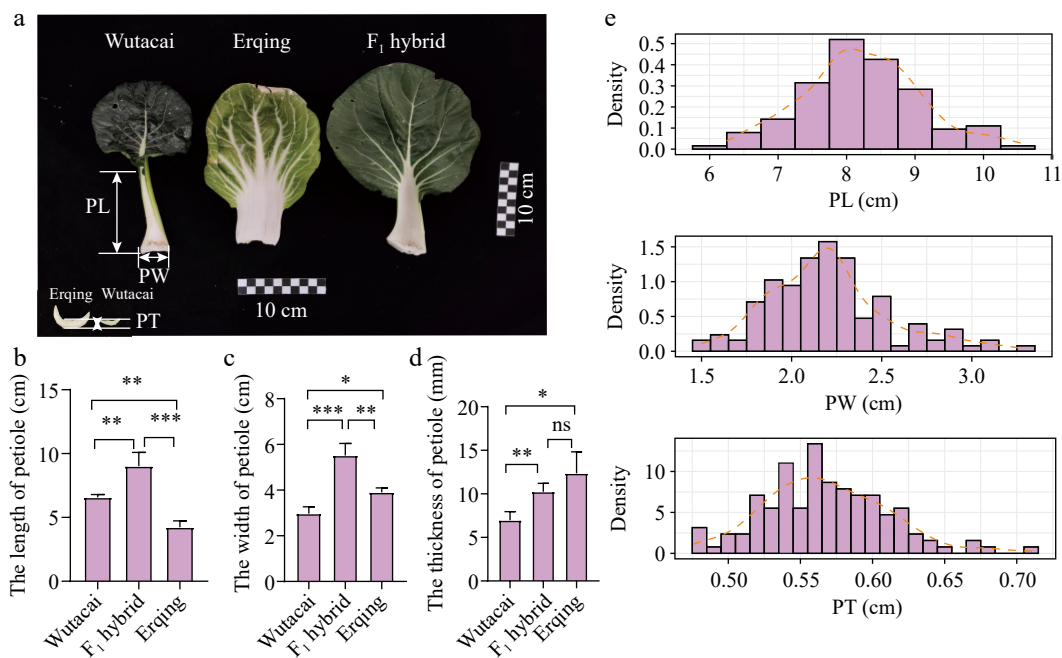


Fig. 1 The performances of Wutacai, Erqing, F₁ hybrid, and RIL population. (a) The appearance of Wutacai, Erqing, and F₁ hybrid. (b) Comparison of PL from Wutacai, Erqing, and F₁ hybrid. (c) Comparison of PW from Wutacai, Erqing, and F₁ hybrid. (d) Comparison of PT from Wutacai, Erqing, and F₁ hybrid. ns indicates no significance. Asterisks(*, **, and ***) indicate $p < 0.05$, $p < 0.01$, and $p < 0.001$. (e) Distribution plots of BLUPs for PL, PW, and PT.

permutations at 0.05 level. The final interval of significant QTL was determined using a 1.5 LOD drop.

Candidate gene analysis

The candidate genes were annotated according to the genome of non-heading Chinese cabbage, which was downloaded from the Non-heading Chinese Cabbage and Watercress Database (http://tbir.njau.edu.cn/NhCCD_bHubs/index.jsp)^[21]. BLASTp with value 1e-5 was used to identify the homologous genes in Arabidopsis. Gene description was downloaded from the TAIR database (www.arabidopsis.org).

RNA isolation and qRT-PCR analysis

The total RNA of petioles in Wutacai and Erqing was isolated using SteadyPure Plant RNA Extraction Kit (Accurate Biology, Changsha, China). RNA was reverse transcribed into cDNA using HiScript IV 1st Strand cDNA Synthesis Kit (+gDNA wiper) (Vazyme, Nanjing, China). ChamQ Blue Universal SYBR qPCR Master Mix (Vazyme, Nanjing, China) was utilized for qRT-PCR analysis. The PCR procedure and calculation of relative expression followed the method of Bai et al.^[18]. The relative primers were designed by SnapGene and listed in [Supplementary Table S1](#).

Results

Performance of petiole in Wutacai and Erqing populations

Wutacai and Erqing, which exhibited different types of petiole, were selected to construct an RIL population for genes associated with petiole exploration ([Fig. 1a](#); [Supplementary Table S2](#)). Wutacai produced slender, narrow, and thin petioles, whereas Erqing exhibited shorter, wider, and thicker petioles ([Fig. 1a](#)). Based on the difference of petioles, PL, PW, and PT were measured in Wutacai, Erqing, and their F_1 hybrid, which came from the crossing of Wutacai and Erqing ([Fig. 1b](#); [Supplementary Table S2](#)). The PL in Erqing was 55.22%–74.60% of that in Wutacai. The PW and PT in Wutacai were 60.23%–80.49%, and 44.79%–66.50% of those in Erqing, respectively ([Fig. 1c, d](#); [Supplementary Table S2](#)). PL and PW in the F_1 hybrid exhibited higher than that in parents, which indicated that PL and PW showed heterosis and overdominance ([Fig. 1b, c](#); [Supplementary Table S2](#)). PT in the F_1 hybrid showed an intermediated level, indicating that PT was an incomplete dominant trait ([Fig. 1d](#); [Supplementary Table S2](#)). The RIL population was cultivated at three locations (Baima, Jurong, and Huzhou). The PL, PW, and PT exhibited normal distribution, which suggested that those traits were controlled by multiple genes ([Fig. 1e](#); [Supplementary Fig. S1](#); [Supplementary Table S2](#)).

Genetic analysis of petiole shape

The phenotypic data collected from three locations were used to construct the best-mixed liner model. The ANOVA analysis revealed that PL, PW, and PT were suitable for the model with genotype and environment as fixed factors and interaction between genotype and environment, repeat in the environment as a random factor, which suggested that PL, PW, and PT were mutually controlled by genotype and environment ([Table 1](#)). Meanwhile, the broad sense heritability (H^2) was also calculated for PL, PW, and PT. The heritability of PL and PW were 0.66 and 0.74, respectively. The high H^2 suggested a dominant effect for PL and PW from genotype ([Table 1](#)). The heritability of PT was 0.44, indicating that PT was not stable and affected easily by environments ([Table 1](#)).

QTL mapping

To obtain the comprehensive QTL, BLUPs and all of the phenotypic data collected from different environments were used for QTL

Table 1. The variance of effect factor and heritability for PL, PW, and PT.

Components	PL	PW	PT
Genotype	1.17946	0.16256	0.00477
Environment	2.87536	0.48803	0.04405
Genotype:environment	0.99288	0.08294	0.01179
Blocks (rep in environment)	0.08763	0.04030	0.00078
Residual	1.37812	0.14696	0.01153
Heritability (H^2)	0.66038	0.74026	0.43340

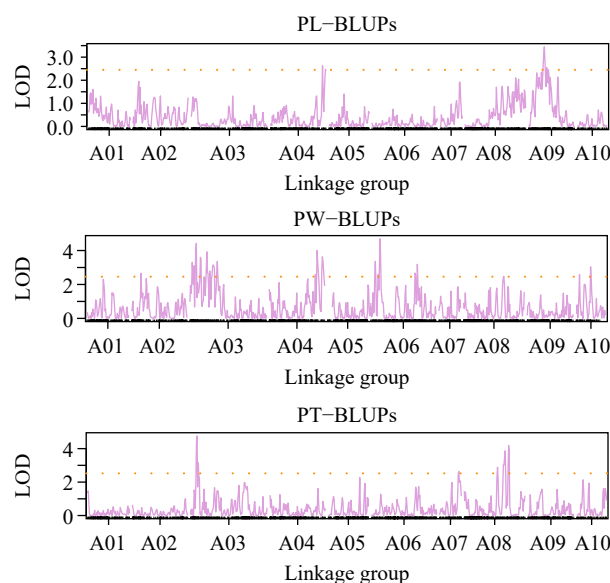


Fig. 2 QTL mapping for BLUP values in PL, PW, and PT.

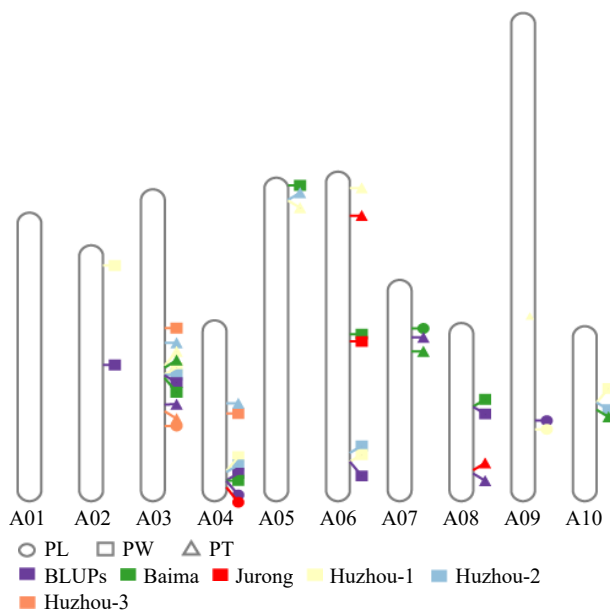


Fig. 3 Physical location of QTL for PL, PW, and PT.

mapping. A total of four QTL were detected in PL and contributed to 10.31%–18.57% phenotypic variance ([Figs 2, 3](#); [Supplementary Fig. S2](#); [Table 2](#); [Supplementary Table S3](#)). *qPLA04.1* and *qPLA09.1* explained the highest phenotypic variance and detected at BLUPs, Jurong, and Huzhou ([Figs 2, 3](#); [Supplementary Fig. S2](#); [Table 2](#); [Supplementary Table S3](#)). *qPLA03.1* and *qPLA07.1* were also detected in Baima and Huzhou ([Figs 2, 3](#); [Supplementary Fig. S2](#); [Table 2](#); [Supplementary Table S3](#)). A total of seven QTL were

Table 2. The QTL detected by BLUPs.

Traits	Locations	Linkage group	Locus	Peak LOD	1.5 LOD interval		Additive effect	Phenotypic variance explained (%)
					Marker right	Marker left		
PL	BLUPs	A04	<i>qPL.A04.1</i>	2.62	A04_20389448	A04_22047361	0.23155	6.056
		A09	<i>qPL.A09.1</i>	3.42	A09_58654691	A09_49099062	−0.26456	9.13
	Baima	A07	<i>qPL.A07.1</i>	2.81	A07_11058656	A07_1764887	0.1465	10.31459
	Jurong	A04	<i>qPL.A04.1</i>	2.77	A04_22095429	A04_22047361	1.0422	14.812217
	Huzhou-1	A09	<i>qPL.A09.1</i>	2.73	A09_59798610	A09_50254249	−0.548	11.37389
PW	BLUPs	A03	<i>qPL.A03.1</i>	3.15	A03_32044940	A03_30518078	−0.5585	10.97715
		A02	<i>qPW.A02.1</i>	2.66	A02_733009	A02_30883969	−0.06004	2.477
	Baima	A03	<i>qPW.A03.1</i>	4.43	A03_31182238	A03_18015813	−0.07582	3.997
		A04	<i>qPW.A04.1</i>	4.01	A04_20233219	A04_22047361	−0.0734	3.967
		A06	<i>qPW.A06.1</i>	4.69	A06_40690069	A06_35966291	−0.09773	6.639
		A08	<i>qPW.A08.1</i>	2.48	A08_517021	A08_21634479	0.05469	2.065
		A03	<i>qPW.A03.1</i>	4.11	A03_31182335	A03_18724031	−0.09117	5.642
		A04	<i>qPW.A04.1</i>	4.20	A04_19732246	A04_22656727	−0.06587	3.099
		A05	<i>qPW.A05.1</i>	3.76	A05_1222122	A05_815039	0.07976	4.678
		A06	<i>qPW.A06.1</i>	4.55	A06_38372945	A06_4564281	−0.07796	4.141
	Jurong	A08	<i>qPW.A08.1</i>	2.90	A08_145893	A08_21920792	0.0713	3.862
		A06	<i>qPW.A06.1</i>	3.23	A06_41497657	A06_3383035	−0.32253	15.489
	Huzhou-1	A02	<i>qPW.A02.1</i>	2.69	A02_130169	A02_5193431	−0.1424	4.59
		A03	<i>qPW.A03.1</i>	3.52	A03_30864524	A03_18015813	−0.10545	2.39
	Huzhou-2	A04	<i>qPW.A04.1</i>	3.22	A04_17762563	A04_22047361	−0.12212	3.436
		A06	<i>qPW.A06.1</i>	3.99	A06_40690069	A06_35966291	−0.1821	7.46
		A10	<i>qPW.A10.1</i>	2.74	A10_1410956	A10_18769214	−0.1114	2.585
		A03	<i>qPW.A03.1</i>	4.28	A03_24356778	A03_24682730	−0.14407	4.007
		A04	<i>qPW.A04.1</i>	3.47	A04_17762563	A04_22312000	−0.15091	4.341
		A06	<i>qPW.A06.1</i>	3.16	A06_38372945	A06_35966291	−0.12281	2.769
		A10	<i>qPW.A10.1</i>	3.15	A10_1410956	A10_18769214	−0.15227	4.242
	Huzhou-3	A03	<i>qPW.A03.1</i>	4.11	A03_18727114	A03_17930086	−0.19753	6.626
		A04	<i>qPW.A04.1</i>	2.67	A04_2530871	A04_22047361	0.19091	5.66
PT	BLUPs	A03	<i>qPT.A03.1</i>	4.76	A03_30621834	A03_26249977	−0.01541	11.31
		A07	<i>qPT.A07.1</i>	2.64	A07_14415306	A07_775788	0.010057	4.7
	Baima	A08	<i>qPT.A08.1</i>	4.2	A08_18588344	A08_21214068	0.014503	10.21
		A03	<i>qPT.A03.1</i>	3.33	A03_30478585	A03_16647267	−0.02032	5.888
		A07	<i>qPT.A07.1</i>	4.14	A07_14441999	A07_4436414	0.021074	5.974
	Jurong	A10	<i>qPT.A10.1</i>	2.52	A10_1739370	A10_20349334	0.014812	2.633
		A06	<i>qPT.A06.1</i>	2.87	A06_7730815	A06_3882585	−0.07958	7.368
	Huzhou-1	A08	<i>qPT.A08.1</i>	2.88	A08_17707535	A08_21175529	0.07518	6.907
		A03	<i>qPT.A03.1</i>	3.19	A03_30864524	A03_15713701	−0.03759	6.163
	Huzhou-2	A05	<i>qPT.A05.1</i>	4.10	A05_4097617	A05_1951585	−0.04991	9.805
		A06	<i>qPT.A06.2</i>	2.93	A06_2453061	A06_1858366	0.03243	4.529
		A03	<i>qPT.A03.1</i>	4.52	A03_21844186	A03_18724031	−0.05279	11.217
		A04	<i>qPT.A04.1</i>	2.47	A04_1147833	A04_20772670	0.03016	3.228
	Huzhou-3	A05	<i>qPT.A05.1</i>	3.26	A05_4097617	A05_1749785	−0.03566	5.048
		A03	<i>qPT.A03.1</i>	7.38	A03_31182238	A03_27499477	−0.07229	19.834

detected for PW and explained 15.49%–45.94% phenotypic variance (Figs 2, 3; Supplementary Fig. S2; Table 2; Supplementary Table S3). *qPW.A03.1*, *qPW.A04.1*, and *qPW.A06.1* were detected in several environments and explained 2.39%–6.63%, 3.10%–5.66%, and 2.77%–15.49% phenotypic variance, respectively (Figs 2, 3; Supplementary Fig. S2; Table 2; Supplementary Table S3). A total of eight QTL were detected in PT and explained 20.76%–31.20% phenotypic variance (Figs 2, 3; Supplementary Fig. S2; Table 2). *qPT.A03.1*, was detected in the majority of environments, was determined as the stable QTL for PT and explained 5.89%–19.83% phenotypic variance (Figs 2, 3; Supplementary Fig. S2; Table 2; Supplementary Table S3). The QTL for PL, PW, and PT were not stable and affected easily by environments.

Moreover, the QTL for PL, PW, and PT were compared, and the study found that *qPL.A03.1*, *qPW.A03.1*, and *qPT.A03.1* shared co-localization and were determined as the same QTL. *qPL.A04.1*, *qPW.A04.1*, and *qPT.A04.1* also shared the same physical position, considering the same QTL (Fig. 3; Supplementary Fig. S2;

Supplementary Table S3). The results suggested that the two QTLs could control PL, PW, and PT simultaneously and showed a predominant effect, regarded as the key QTL for petioles shape. *qPL.A07.1* and *qPT.A07.1* were considered as the same QTL and showed similar localization, which indicated that the QTL was responsible for PL and PT simultaneously (Fig. 3; Supplementary Fig. S2; Supplementary Table S3). *qPW.A05.1*, *qPW.A06.1*, *qPW.A08.1*, and *qPW.A10.1* were co-localized with *qPT.A05.1*, *qPT.A06.1*, *qPT.A08.1*, and *qPT.A10.1* respectively, which indicated that the four QTL were responsible for PW and PT simultaneously (Fig. 3; Supplementary Fig. S2; Supplementary Table S3).

Effect analysis of QTL

The additive effect was analyzed to understand the effect of QTL further. *qPL.A03.1*, *qPW.A03.1*, and *qPT.A03.1* showed a negative additive effect, signifying the contributions for slender, wider, and thicker petiole from the Erqing allele (AA) (Fig. 4; Supplementary Table S3). *qPL.A04.1* and *qPT.A04.1* exhibited positive additive

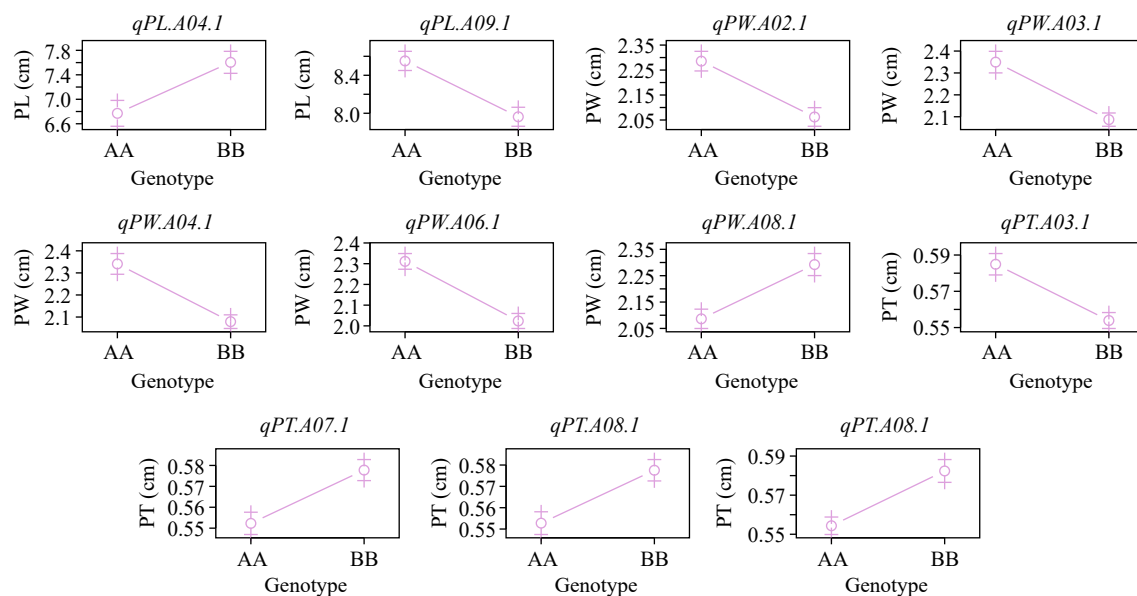


Fig. 4 The effect plot of QTL detected by BLUPs.

effects, whereas *qPW.A04.1* showed negative additive effect, which suggested that the Wutacai allele (BB) contributed to slender and thicker petiole and contributions from the Erqing allele led to wider petiole (Fig. 4; Supplementary Table S3). Apart from the two crucial intervals, The QTL on chromosome A05 showed positive additive effects in PW and negative additive effects in PT, signifying that the Wutacai allele contributed to wider and thinner petiole (Fig. 4; Supplementary Table S3). *qPW.A06.1* and *qPT.A06.1* showed negative additive effects, which indicated that contribution for wider and thicker petiole from the Erqing allele (Fig. 4; Supplementary Table S3). *qPW.A08.1* and *qPT.A08.1* showed positive additive effects, which indicated that contribution for wider and thicker petiole from the Wutacai allele (Fig. 4; Supplementary Table S3). *qPW.A10.1* showed a positive additive effect, signifying contribution for wider petiole from Wutacai, whereas *qPT.A10.1* showed a negative additive effect, suggesting contribution for thicker petiole from Erqing (Fig. 4; Supplementary Table S3). *qPL.A10.1* and *qPT.A10.1* showed a positive additive effect, which indicated that contribution for slender and thicker petiole from the Wutacai allele (Fig. 4; Supplementary Table S3).

Candidate genes analysis

The QTL detected on chromosomes A03 and A04 were considered the most important QTL for petiole development. The *qPL.A03.1*, *qPW.A03.1*, and *qPT.A03.1* were annotated based on NHCC001 genome^[21]. The candidate genes were screened by gene description, and 12 candidate genes associated with leaf and petiole development were obtained (Table 3). *BraC03g067590*, homologue of *ABNORMAL LEAF-SHAPE 1* (*ALE1*), the mutant exhibited shorter petiole^[22]. *BraC03g044910* was a member of the NAC transcription factor family, named *NAC036*; overexpression of *NAC036* in *Arabidopsis thaliana* led to shorter petiole length^[23]. *BraC03g037400*, *BraC03g049640* and *BraC03g045390*, homologues of *TCP4*, *TCP2* and *TCP5*, participated in leaf differentiation^[24–26]. Two candidate genes (*IAA31* and *IPT8*) related to IAA and cytokinin also may play a role in petiole development^[27,28]. *BraC03g050770* and *BraC03g063060* were homologous with *BARELY ANY MERISTEM 3* (*BAM3*) and *ROTUNDIFOLIA 3* (*ROT3*), which involved in controlling leaf shape^[29,30]. *GRF2* (*BraC03g064340*) and *GRF5* (*BraC03g036830*) were also annotated, and the two genes were related to plant growth and may function in petiole and leaf development^[31,32]. Two

reliable genes associated with petiole development were screened in *qPL.A04.1*, *qPW.A04.1*, and *qPT.A04.1*. *BraC04g031470* was homologous with *BLADE ON PETIOLE2* (*BOP2*), which mutant in *Arabidopsis* exhibited short petiole^[33]. *BraC04g031910* was annotated as *SQUAMOSA PROMOTER BINDING PROTEIN-LIKE 9* (*SPL9*), which showed genetic interaction with *BOP2*^[33].

The qRT-PCR analysis was adopted to further identify the candidate genes. The expression levels of six candidate genes (*BcNAC036*, *BcIAA31*, *BcBLI*, *BcTCP2*, *BcBOP2*, and *BcSPL9*) were detected in petioles of parental lines, and others were not, suggesting the association between these genes and petiole development (Fig. 5). The expression levels of *BcBLI* and *BcSPL9* showed no significant difference between Wutacai and Erqing, which indicated that the two genes were not related to petiole shape (Fig. 5). The expression levels of *BcNAC036*, *BcIAA31*, *BcTCP2*, and *BcBOP2* in Wutacai were higher than that in Erqing (Fig. 5). Especially, the expression levels of *BcIAA31* and *BcBOP2* in Wutacai were approximately five folds of those in Erqing (Fig. 5). The results revealed that *BcNAC036*, *BcIAA31*, and *BcTCP2* may be the major candidate genes in *qPL.A03.1*, *qPW.A03.1*, and *qPT.A03.1*, and *BcIAA31* was the promise candidate genes. *BcBOP2* was the promising candidate gene in *qPL.A04.1*, *qPW.A04.1*, and *qPT.A04.1*.

Discussion

Petiole is an important edible organ, and the petiole shape gradually becomes one of the traits of concern in NHCC. With the improvement of people's living standards, the requirement for quality of vegetables is increasing, and the vegetables with specific characteristics are needed, such as NHCC with short and slimmer petioles as leafy varieties and NHCC with length, wide and thick petiole as petiole variety. Thus, understanding the genetic model and exploration of candidate genes for petiole development and shape are required for germplasm enhancement of breeding in NHCC.

In this study, two varieties were adopted, showing significant differences in petiole length, width, and thickness in different environments, to construct a RIL population for genetic analysis and QTL mapping (Fig. 1a; Supplementary Table S2). Genetic analysis showed that PL, PW, and PT were dominant traits and controlled by multiple genes, which was similar to previous studies^[15–17]. Meanwhile, the

Table 3. The reliable candidate genes annotated in QTL on chromosomes A03 and A04.

ID	Chromosomes	Candidate genes	Homologue in <i>Arabidopsis</i>	Gene name	Ref.
P1	A03	<i>BraC03g067590</i>	<i>AT1G62340.1</i>	<i>ALE1</i>	[22]
P2	A03	<i>BraC03g044910</i>	<i>AT2G17040.1</i>	<i>NAC036</i>	[23]
P3	A03	<i>BraC03g036830</i>	<i>AT3G13960.1</i>	<i>GRF5</i>	[31]
P4	A03	<i>BraC03g064340</i>	<i>AT4G37740.1</i>	<i>GRF2</i>	[32]
P5	A03	<i>BraC03g037400</i>	<i>AT3G15030.3</i>	<i>TCP4</i>	[26]
P6	A03	<i>BraC03g038570</i>	<i>AT3G17600.1</i>	<i>IAA31</i>	[27]
P7	A03	<i>BraC03g039350</i>	<i>AT3G19160.1</i>	<i>IPT8</i>	[28]
P8	A03	<i>BraC03g042250</i>	<i>AT3G23980.1</i>	<i>BLI</i>	[34]
P9	A03	<i>BraC03g049640</i>	<i>AT4G18390.2</i>	<i>TCP2</i>	[24]
P10	A03	<i>BraC03g050770</i>	<i>AT4G20270.1</i>	<i>BAM3</i>	[30]
P11	A03	<i>BraC03g063060</i>	<i>AT4G36380.1</i>	<i>ROT3</i>	[29]
P12	A03	<i>BraC03g045390</i>	<i>AT5G60970.1</i>	<i>TCP5</i>	[25]
P13	A04	<i>BraC04g031470</i>	<i>AT2G41370.1</i>	<i>BOP2</i>	[33]
P14	A04	<i>BraC04g031910</i>	<i>AT2G42200.1</i>	<i>SPL9</i>	[33]

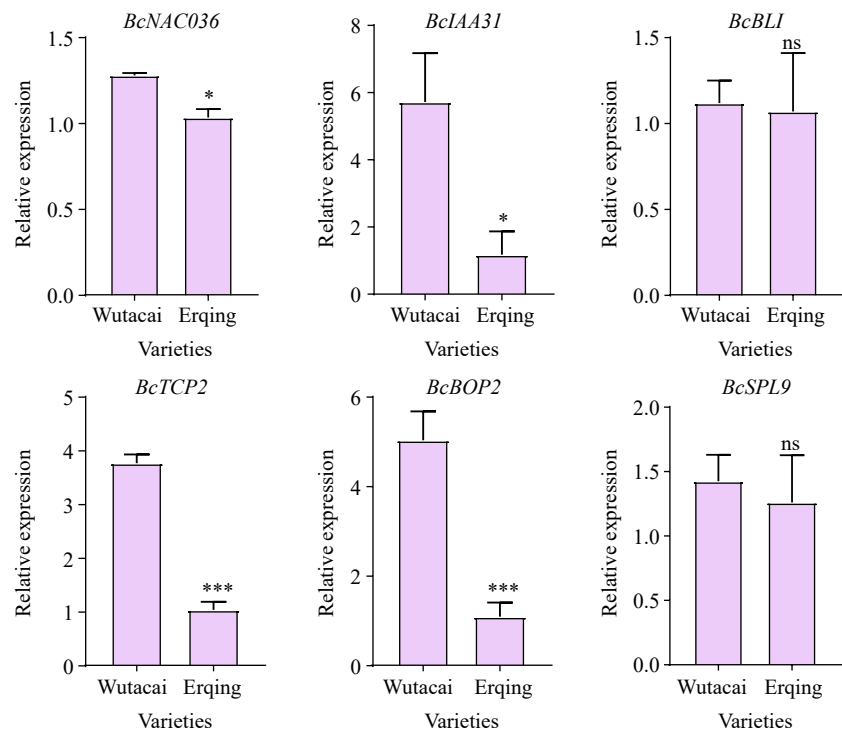


Fig. 5 qRT-PCR analysis of candidate genes in Wutacai and Erqing.

broad sense heritability of PL, PW, and PT were 0.66, 0.74, and 0.43 respectively (Table 1). Previous studies have illustrated the heritability of PL, PW, and PT as 0.33, 0.41, and 0.33, respectively, by another RIL population^[17]. The low heritability of the two studies illustrated that the three traits were easily affected by the environment.

The four QTLs for PL were identified on chromosomes A03, A04, A07, and A09, which showed little difference from previous studies^[15–17]. The three QTLs were identified in Wutacai and Chinese cabbage populations and distributed on chromosomes A01 and A06^[16]. The four QTLs were identified in Maertou and Suzhouqing populations and distributed in A08 and A09^[17]. The QTL on chromosome A09 was compared and illustrated that the *qPL.A09.1* (49.10–59.80 Mb) shared physical localization with the two QTLs identified in Maertou and Suzhouqing population (*qPL.9.2*, 55.24–55.38 Mb; *qPL.9.1*, 55.97–55.61 Mb)^[17]. The comparison indicated that *qPL.A09.1* may be stable QTL for NHCC accessions, which could be utilized for molecular marker development and explore the core genes for PL. The QTL for PW was identified on chromosomes A02, A03, A04, A05, A06, A08, and A10 in our study (Supplementary

Table S3), which were not detected in previous studies. The new QTL may contribute to obtaining new genes for controlling PW. QTL on chromosomes A03 and A04 were mutually detected in all three traits, including PL, PW, and PT. The results indicate that the two QTL can regulate PL, PW and PT, PL, PW, and PT simultaneously, suggesting pleiotropic effects and linkage among the traits related to petiole shape (Supplementary Table S3). The relationship was beneficial in developing molecular markers that could identify three traits simultaneously, improving the efficiency of the breeding process. Moreover, QTL on chromosome A04 showed different additive effects for PL, PW, and PT. *qPL.A04.1* and *qPT.A04.1* performed a positive additive effect, which indicated that the allele from Erqing contributed to longer and thicker petiole, whereas *qPW.A04.1* showed a negative additive effect, which indicated that the allele from Wutacai contributed to narrow petiole (Fig. 3; Supplementary Table S3). The same QTL showed opposing effect for different traits, which may make it difficult to breed a single trait. The same QTL may imply the same genes controlled for three traits, which indicates that the genes may participate upstream of a regulatory

pathway or play an important role in mediating phytohormone. The potential regulatory network could be studied in the future.

A total of 14 reliable candidate genes were obtained, and the qRT-PCR analysis further identified *BcIAA31* and *BcBOP2* as the promising candidate genes in QTL on chromosomes A03 and A04, respectively (Fig. 5; Table 3). A total of five candidate genes were screened for PL, PW, and PT, and obtained one candidate gene for PL in a previous study^[17]. From those candidate genes, *BOP* and *IAA* genes are annotated in the Wutacai and Erqing populations and the Maertou and Suzhouqing populations^[17]. *BOP1* and *IAA19* are annotated in Maertou and Suzhouqing populations, and *BOP2* and *IAA31* were annotated in Wutacai and Erqing populations (Table 3). *BOP1* is a promising candidate gene in *qPL.9.2* mapped in Maertou and Suzhouqing populations, which share physical location with *qPLA09.1* in this study, which further revealed the essential roles in petiole shape. *BOP1* and *BOP2* are BTB-ankyrin proteins and are involved in plant architecture^[35]. In *Arabidopsis*, *bop1bop2* mutant results in loss of petiole^[35,36]. During vegetative development, *BOP1* and *BOP2* are transcriptional coactivators in shoot apical meristem and participate in leaf morphogenesis and floral induction^[37,38]. Thus, *BOP* genes may be the important regulator for petiole development and petiole shape. *IAA19* and *IAA31* are members of the Aux/IAA family of proteins, and they respond to auxin signaling and can simultaneously control PL, PW, and PT^[39]. Auxin is an important phytohormone and promotes cell proliferation and cell elongation^[40]. *IAA19* and *IAA31* can regulate hypocotyls growth^[41–43]. However, the function of these genes in NHCC has not been identified.

Author contributions

The authors confirm contribution to the paper as follows: study conception and design: Li Ying, Bai A, Chen Z, data collection: Zhao T, Zhang F, Li Yan, analysis and interpretation of results: Chen Z, Liu T, Bai A, Wang X, manuscript revision: Chen Z, Bai A, Hou X. All authors reviewed the results and approved the final version of the manuscript.

Data availability

The datasets generated during and/or analyzed during the current study are available from the corresponding author upon reasonable request.

Acknowledgments

This work was supported by the National Natural Science Foundation of China (Grant No. 32172565), Earmarked Fund for China Agriculture Research System (Grant No. CARS-23-A-16), Jiangsu Seed Industry Revitalization Project (Grant No. JBGS (202015)), and the Bioinformatics Center of Nanjing Agricultural University.

Conflict of interest

The authors declare that they have no conflict of interest.

Supplementary information accompanies this paper at (<https://www.maxapress.com/article/doi/10.48130/vegres-0025-0014>)

Dates

Received 20 February 2025; Revised 16 April 2025; Accepted 13 May 2025; Published online 13 June 2025

References

- Hou X, Li Y, Liu T. 2022. Advances in genetic breeding and molecular biology of non-heading Chinese cabbage. *Journal of Nanjing Agricultural University* 45(05):864–73
- Gebauer R, Vanbeverem SPP, Volařík D, Plichta R, Ceulemans R. 2016. Petiole and leaf traits of poplar in relation to parentage and biomass yield. *Forest Ecology and Management* 362:1–9
- Weijsschedé J, Antonise K, de Caluwe H, de Kroon H, Huber H. 2008. Effects of cell number and cell size on petiole length variation in a stoloniferous herb. *American Journal of Botany* 95:41–49
- Damayanthi, Ranwala NK, Decoteau DR, Ranwala AP, Miller WB. 2002. Changes in soluble carbohydrates during phytochrome-regulated petiole elongation in watermelon seedlings. *Plant Growth Regulation* 38:157–63
- Devlin PF, Robson PR, Patel SR, Goosey L, Sharrock RA, et al. 1999. Phytochrome D acts in the shade-avoidance syndrome in *Arabidopsis* by controlling elongation growth and flowering time. *Plant Physiology* 119:909–15
- Nishizawa T. 1990. Effects of daylength on cell length and cell number in strawberry petioles. *Journal of the Japanese Society for Horticultural Science* 59:533–38
- Hamasaki H, Ayano M, Nakamura A, Fujioka S, Asami T, et al. 2020. Light activates brassinosteroid biosynthesis to promote hook opening and petiole development in *Arabidopsis thaliana*. *Plant and Cell Physiology* 61(7):1239–51
- Küpers JJ, Snoek BL, Oskam L, Pantazopoulou CK, Matton SEA, et al. 2023. Local light signaling at the leaf tip drives remote differential petiole growth through auxin-gibberellin dynamics. *Current Biology* 33(1):75–85.e5
- Kilen TC. 1983. Inheritance of a short petiole trait in soybean. *Crop Science* 23:1208–10
- Nagatani A, Chory J, Furuya M. 1991. Phytochrome B is not detectable in the hy3 mutant of *Arabidopsis*, which is deficient in responding to end-of-day far-red light treatments. *Plant and Cell Physiology* 32:1119–22
- Reed JW, Nagpal P, Poole DS, Furuya M, Chory J. 1993. Mutations in the gene for the red/far-red light receptor phytochrome B alter cell elongation and physiological responses throughout *Arabidopsis* development. *The Plant Cell* 5:147–57
- Tsukaya H, Kozuka T, Kim GT. 2002. Genetic control of petiole length in *Arabidopsis thaliana*. *Plant and Cell Physiology* 43:1221–28
- Liu Z, She H, Xu Z, Zhang H, Li G, et al. 2021. Quantitative trait loci (QTL) analysis of leaf related traits in spinach (*Spinacia oleracea* L.). *BMC Plant Biology* 21:290
- Huang J, Sun J, Liu E, Yuan S, Liu Y, et al. 2021. Mapping of QTLs detected in a broccoli double diploid population for planting density traits. *Scientia Horticulturae* 277:109835
- McCammon KR, Honma S. 1986. The inheritance of petiole characteristics in Pak-Choi. *Scientia Horticulturae* 28:29–35
- Li F, Liu Z, Chen H, Wu J, Cai X, et al. 2023. QTL mapping of leaf-related traits using a high-density Bin map in *Brassica rapa*. *Horticulturae* 9:433
- Zhao T, Bai A, Wang X, Zhang F, Yang M, et al. 2024. Genetic mapping for leaf shape and leaf size in non-heading Chinese cabbage by a RIL population. *Horticulturae* 10:529
- Bai A, Zhao T, Li Y, Zhang F, Wang H, et al. 2024. QTL mapping and candidate gene analysis reveal two major loci regulating green leaf color in non-heading Chinese cabbage. *Theoretical and Applied Genetics* 137:105
- Arends D, Prins P, Jansen RC, Broman KW. 2010. R/qtl: high-throughput multiple QTL mapping. *Bioinformatics* 26:2990–92
- Broman KW, Gatti DM, Simecek P, Furlotte NA, Prins P, et al. 2019. R/qtl2: software for mapping quantitative trait loci with high-dimensional data and multiparent populations. *Genetics* 211:495–502
- Li Y, Liu GF, Ma LM, Liu TK, Zhang CW, et al. 2020. A chromosome-level reference genome of non-heading Chinese cabbage [*Brassica campestris* (syn. *Brassica rapa*) ssp. *chinensis*]. *Horticulture Research* 7:212
- Tanaka H, Watanabe M, Sasabe M, Hiroe T, Tanaka T, et al. 2007. Novel receptor-like kinase ALE2 controls shoot development by specifying epidermis in *Arabidopsis*. *Development* 134:1643–52

23. Kato H, Motomura T, Komeda Y, Saito T, Kato A. 2010. Overexpression of the NAC transcription factor family gene *ANAC036* results in a dwarf phenotype in *Arabidopsis thaliana*. *Journal of Plant Physiology* 167:571–77
24. He Z, Zhou X, Chen J, Yin L, Zeng Z, et al. 2021. Identification of a consensus DNA-binding site for the TCP domain transcription factor *TCP2* and its important roles in the growth and development of *Arabidopsis*. *Molecular Biology Reports* 48:2223–33
25. Yu H, Zhang L, Wang W, Tian P, Wang W, et al. 2021. *TCP5* controls leaf margin development by regulating *KNOX* and *BEL*-like transcription factors in *Arabidopsis*. *Journal of Experimental Botany* 72:1809–21
26. Baulies JL, Bresso EG, Goldy C, Palatnik JF, Schommer C. 2022. Potent inhibition of TCP transcription factors by miR319 ensures proper root growth in *Arabidopsis*. *Plant Molecular Biology* 108:93–103
27. Sato A, Yamamoto KT. 2008. Overexpression of the non-canonical *Aux/IAA* genes causes auxin-related aberrant phenotypes in *Arabidopsis*. *Physiologia Plantarum* 133:397–405
28. Wang Y, Shen W, Chan Z, Wu Y. 2015. Endogenous cytokinin overproduction modulates ROS homeostasis and decreases salt stress resistance in *Arabidopsis thaliana*. *Frontiers in Plant Science* 6:1004
29. Lee YK, Kim IJ. 2018. Functional conservation of *Arabidopsis* *LNG1* in tobacco relating to leaf shape change by increasing longitudinal cell elongation by overexpression. *Genes & Genomics* 40:1053–62
30. Wang Q, Aliaga Fandino AC, Graeff M, DeFalco TA, Zipfel C, et al. 2023. A phosphoinositide hub connects CLE peptide signaling and polar auxin efflux regulation. *Nature Communications* 14:423
31. Beltramino M, Debernardi JM, Ferela A, Palatnik JF. 2021. *ARF2* represses expression of plant *GRF* transcription factors in a complementary mechanism to microRNA *miR396*. *Plant Physiology* 185:1798–812
32. Beltramino M, Ercoli MF, Debernardi JM, Goldy C, Rojas AML, et al. 2018. Robust increase of leaf size by *Arabidopsis thaliana* *GRF3*-like transcription factors under different growth conditions. *Scientific Reports* 8:13447
33. Hu T, Manuela D, Xu M. 2023. *SQUAMOSA* PROMOTER BINDING PROTEIN-LIKE 9 and 13 repress *BLADE-ON-PETIOLE 1* and 2 directly to promote adult leaf morphology in *Arabidopsis*. *Journal of Experimental Botany* 74:1926–39
34. Yang R, Liu P, Zhang T, Dong H, Jing Y, et al. 2023. Plant-specific *BLISTER* interacts with kinase *BIN2* and *BRASSINAZOLE RESISTANT1* during skotomorphogenesis. *Plant Physiology* 193:1580–96
35. Khan M, Xu H, Hepworth SR. 2014. *BLADE-ON-PETIOLE* genes: setting boundaries in development and defense. *Plant Science* 215–216:157–71
36. Wang Y, Salasini BC, Khan M, Devi B, Bush M, et al. 2019. Clade I TGACG-motif binding basic leucine zipper transcription factors mediate *BLADE-ON-PETIOLE*-dependent regulation of development. *Plant Physiology* 180:937–51
37. Xing Q, Creff A, Waters A, Tanaka H, Goodrich J, et al. 2013. *ZHOUP1* controls embryonic cuticle formation via a signalling pathway involving the subtilisin protease *ABNORMAL LEAF-SHAPE1* and the receptor kinases *GASSHO1* and *GASSHO2*. *Development* 140:770–79
38. Andrés F, Romera-Branchat M, Martínez-Gallegos R, Patel V, Schneeberger K, et al. 2015. Floral induction in *Arabidopsis* by *FLOWERING LOCUS T* requires direct repression of *BLADE-ON-PETIOLE* genes by the homeodomain protein *PENNYWISE*. *Plant Physiology* 169:2187–99
39. Jain M, Kaur N, Garg R, Thakur JK, Tyagi AK, et al. 2006. Structure and expression analysis of early auxin-responsive *Aux/IAA* gene family in rice (*Oryza sativa*). *Functional & Integrative Genomics* 6:47–59
40. Bishop GJ, Koncz C. 2002. Brassinosteroids and plant steroid hormone signaling. *The Plant Cell* 14:S97–S110
41. Tatematsu K, Kumagai S, Muto H, Sato A, Watahiki MK, et al. 2004. *MASSUGU2* encodes *Aux/IAA19*, an auxin-regulated protein that functions together with the transcriptional activator *NPH4/ARF7* to regulate differential growth responses of hypocotyl and formation of lateral roots in *Arabidopsis thaliana*. *The Plant Cell* 16:379–93
42. Zhou XY, Song L, Xue HW. 2013. Brassinosteroids regulate the differential growth of *Arabidopsis* hypocotyls through auxin signaling components *IAA19* and *ARF7*. *Molecular Plant* 6:887–904
43. Lee N, Hwang DY, Lee HG, Hwang H, Kang HW, et al. 2024. *ASYMMETRIC LEAVES1* promotes leaf hyponasty in *Arabidopsis* by light-mediated auxin signaling. *Plant Physiology* 197:kiae550



Copyright: © 2025 by the author(s). Published by Maximum Academic Press, Fayetteville, GA. This article is an open access article distributed under Creative Commons Attribution License (CC BY 4.0), visit <https://creativecommons.org/licenses/by/4.0/>.